The Journal of Immunology

RESEARCH ARTICLE | JULY 01 2001

B-Myb Overexpression Results in Activation and Increased Fas/Fas Ligand-Mediated Cytotoxicity of T and NK Cells[1]

Mark A. Powzaniuk; ... et. al

J Immunol (2001) 167 (1): 242–249.
https://doi.org/10.4049/jimmunol.167.1.242

B-Myb Overexpression Results in Activation and Increased Fas/Fas Ligand-Mediated Cytotoxicity of T and NK Cells[1]

Mark A. Powzaniuk,* Rossana Trotta,* Matthew J. Loza,* Amy Harth,* Renato V. Iozzo,† Lawrence C. Eisenlohr,* Bice Perussia,* and Bruno Calabretta[2]*

The human B-*myb* gene encodes a transcriptional regulator that plays an important role in cell cycle progression, differentiation, and survival. To assess the in vivo role of B-*myb*, we investigated the phenotype of mouse transgenic lines in which B-Myb expression in lymphoid tissues was driven by the LCK proximal promoter. Overexpression of B-Myb had no measurable effect on the subsets of splenic and thymic lymphocytes, but was associated with increased expression of Fas ligand in NK and T cells. B-Myb-overexpressing splenocytes expressed higher IFN-γ levels and contained higher percentages of cytokine-producing cells than wild-type (wt) splenocytes, as detected by Western blot analysis and ELISPOT assays, respectively. Ex vivo-cultured transgenic thymocytes and splenocytes had decreased survival compared with the corresponding cells from wt mice, possibly dependent on increased expression of Fas ligand. In addition, Fas ligand-dependent cytotoxicity of transgenic T and NK cells was significantly higher than that mediated by their wt counterparts. Together, these results indicate that B-Myb overexpression results in T and NK cell activation and increased cytotoxicity. Therefore, in addition to its well-established role in proliferation and differentiation, B-myb also appears to be involved in activation of NK and T cells and in their regulation of Fas/Fas ligand-mediated cytotoxicity *The Journal of Immunology,* **2001, 167: 242–249.**

B-Myb is a widely expressed transcriptional regulator that belongs to the Myb family of DNA-binding proteins. The myb gene family consists of three members: c-myb, the homologue of the transforming gene of the avian myeloblastosis virus, and the myb-related A-myb and B-myb (1, 2). Myb proteins possess three functional domains: a highly conserved and almost identical NH_2-terminal DNA-binding domain recognizing the consensus sequence PyAACG/TG, a central acidic transcriptional activation domain only partially conserved among the family members, and a COOH-terminal negative regulatory domain that functions as a transcriptional repressor (1, 3). Cell cycle-dependent phosphorylation of A- and B-Myb, but not c-Myb, by cyclin A/cdk2 or cyclin E/cdk2 appears to relieve this repression (4, 5). Potential Myb binding sites have been identified in several genes transcriptionally regulated by products of the myb gene family (5). DNA binding-dependent transcriptional regulation by c-Myb has been demonstrated in few cases, whereas it is unclear whether the effect of B-Myb on the promoter activity of B-Myb itself, c-Myc, Bcl-2, 70-kDa heat shock protein, and cdc2 depends on binding to Myb binding sites (4).

B-myb is ubiquitously expressed, whereas c-myb and especially A-myb have a rather restricted tissue-specific expression (4, 5). The pattern of expression of *myb* family genes is reflected in the developmental abnormalities of the corresponding knockout (KO)[3] mice (6–8). A-myb and c-myb KO mice are characterized by defective spermatogenesis and hemopoiesis, respectively (6, 7); by contrast, B-myb is required for proliferation of early stage embryonic cells (8). Although it was speculated that B-myb functions in place of c-myb in nonhemopoietic tissues, B-myb expression within hemopoietic tissues, and its apparent inability to compensate for the hemopoiesis-specific phenotype of c-Myb KO mice is inconsistent with functional redundancy (9). B-myb is expressed in proliferating cells at the G_1/S phase boundary and plays an important role in cell cycle regulation (10). B-myb overexpression reduces the growth factor requirements of transfected BALB/3T3 mouse fibroblasts, stimulates cell cycle progression, and can overcome a p53-induced cell cycle arrest in G_1 (11, 12). In addition, BALB/c-3T3 fibroblasts overexpressing B-myb exhibit a partially transformed phenotype and grow efficiently in soft agar (11).

Levels of endogenous B-myb are down-modulated during differentiation, while its ectopic expression blocks IL-6-mediated differentiation of M1 myeloid leukemic cells (13). Assessment of the role of B-myb in apoptotic processes has resulted in contradictory results. Overexpression of B-myb enhanced the survival of neuroblastoma and a murine cytotoxic T cell line (CTLL-2) while accelerating the apoptosis of M1 cells (14–16).

We report here that transgenic (tg) B-myb expression in vivo results in decreased survival of T cells and increased Fas ligand (FasL) and IFN-γ expression. The latter, together with increased cytotoxicity of transgenic T and NK cells, supports B-myb-related activation in these mice.

Materials and Methods

Transgenic mice

All animals were bred and maintained in a pathogen-free environment at the Kimmel Cancer Center, Thomas Jefferson University (Philadelphia,

*Department of Microbiology and Immunology, Kimmel Cancer Center, and †Department of Pathology and Cell Biology, Jefferson Medical College, Philadelphia, PA 19107

Received for publication January 10, 2001. Accepted for publication April 30, 2001.

The costs of publication of this article were defrayed in part by the payment of page charges. This article must therefore be hereby marked *advertisement* in accordance with 18 U.S.C. Section 1734 solely to indicate this fact.

[1] This work was supported in part by National Institutes of Health grants (to B.C., B.P., L.C.E., and R.V.I.). M.A.P. and M.J.L. were supported in part by Training Grants 5T32HL0778007 and 5T32CA09683, respectively.

[2] Address correspondence and reprint requests to Dr. Bruno Calabretta, Kimmel Cancer Institute, Thomas Jefferson University, 233 South 10th Street, Room 630, Philadelphia, PA 19107. E-mail address: bruno.calabretta@mail.tju.edu

[3] Abbreviations used in this paper: KO, knockout; tg, transgenic; wt, wild type; FasL, Fas ligand; rhFas, recombinant human Fas; PFP, perforin; NKT, $CD3^+$/Pan-NK^+ cells.

0022-1767/01/$02.00

PA). C57BL/6 mice were purchased from The Jackson Laboratory (Bar Harbor, ME). All animal protocols were approved by the institutional animal care and use committee, and National Institutes of Health guidelines for animal care were followed throughout.

The construct LCK-B-myb was generated by insertion of a 2.4-kb fragment containing the coding region of human B-myb cDNA. The B-myb cDNA was released from plasmid LXSN-B-myb (14) following digestion with *Bam*HI and was subcloned into the unique *Bam*HI cloning site downstream from the LCK promoter (17). The 3′-untranslated region of this construct contains introns, exons, and poly(A) addition sites from the human growth hormone gene. The 7.7-kb LCK-B-myb fragment digested with *Sfi*I was used for microinjection (Kimmel Cancer Center, Transgenic Animal Facility) into blastocysts from B6/C3F2.

Transgenic animals were generated according to standard procedures (18). Transgenic progeny were identified by Southern blotting of *Eco*RI-digested tail DNA using the entire 7.7-kb LCK-B-myb fragment as a probe. Murine tg lines were generated after seven backcrosses to C57BL/6 mice.

Histological analysis

This was performed on thymus, spleen, and lymph nodes. All tissues were fixed in 10% buffered formalin, embedded in paraffin, sectioned, and examined microscopically after staining with hematoxylin/eosin using standard procedures.

Cell preparation and culture

Thymus and spleen from 4- to 8-wk-old animals were minced to generate single-cell suspensions in RPMI 1640 medium containing 10% heat-inactivated FBS (Sigma, St. Louis, MO), 1% L-glutamine, and penicillin/streptomycin (100 μg/ml each; Life Technologies, Gaithersburg, MD). The cell suspension was filtered through a nylon mesh, and erythrocytes were lysed with RBC lysis buffer (0.15 M NH_4Cl, 0.01 M $KHCO_3$, and 0.1 mM EDTA, pH 7.3) for 5 min on ice. After washing twice in PBS, B cells from single splenic cell suspensions were removed by panning (19, 20). For this, Kirby-Bauer plates were coated with goat IgG anti-mouse IgG (1/100 in PBS; Cappel) for 1 h at room temperature and washed three times with PBS. Protein-free binding sites were blocked upon incubation with PBS/0.1% BSA for at least 1 h. The splenic cell suspensions ($20–30 \times 10^6$ cells/plate) were incubated for 1 h at 4°C, after which the nonadherent cells were collected and resuspended in RPMI 1640. T cells were isolated from the B cell-depleted populations by negative selection after sensitization with rat anti-mouse Pan-NK mAb (BD PharMingen, San Diego, CA) and panning as described above. Optilux petri dishes (BD Biosciences, Franklin Lakes, NJ) were coated with goat IgG anti-rat IgG $F(ab')_2$ (10 μg/ml, 50 mM Tris, pH 9.5), thus recognizing all Ig classes. Cell viability (trypan blue exclusion) was always ≥90%.

NK cell populations were isolated from B cell-depleted splenic cell suspensions by cell sorting after incubation with anti-mouse Pan-NK mAb (BD PharMingen). Macrophages were isolated from peritoneal lavage. Briefly, RPMI 1640 was used to flush the peritoneal cavity, cells were plated on petri dishes for 1 h at room temperature, and the adherent cells were collected and resuspended in RPMI 1640. Bone marrow cells were isolated from mouse femurs. Dissected femurs were flushed with RPMI 1640 using a syringe, and cells were washed twice and resuspended in RPMI 1640. Peripheral blood was isolated from mice using intracardiac puncture according to standard procedures (21, 22).

Flow cytometry and cell cycle analysis

For cell cycle analysis, 10^6 freshly isolated cells (from thymus and spleen as indicated) were washed once in PBS and fixed in 70% ethanol for at least 30 min at 4°C. Cells were then centrifuged and resuspended in 300 μl PBS containing 50 μg/ml propidium iodide and 2 μg/ml RNase A. After incubation at 37°C for 30 min, cells were analyzed on a Coulter EPICS XL-MCL (Beckman-Coulter, Miami, FL). For flow cytometric analysis, single-cell suspensions (10^5–10^6 cells) were incubated with the indicated mAb for 30 min at 4°C in incubation buffer (0.02% sodium azide and 1% BSA in PBS). Cells were then washed three times in incubation buffer and fixed in 1% formaldehyde. Analysis was performed on a Coulter EPICS XL-MCL and reanalyzed with WinMDI (Joseph Trotter, Scripps Research Institute, La Jolla, CA) software. For cell sorting, freshly isolated cells were treated as described above and resuspended (2×10^7/ml) in RPMI 1640 containing 2% FBS. Cell sorting was performed on a Coulter EPICS ELITE-ESP, and the sorted cells were collected in RPMI 1640 containing 10% FBS. The Abs used were FITC anti-CD8 (53-6.7) and Pan-NK (DX-5), PE anti-CD4 (RM4-5) and anti-B220 (RA3-6B2), CyChrome-conjugated anti-CD3/molecular complex (17A2), and isotype- or Ig class-matched Ab as negative controls for each (BD PharMingen). Sorted populations were >90% homogenous for CD3 or Pan-NK expression as detected on reanalysis.

RNA isolation and Northern blot analysis

Total RNA was isolated from animal tissues, peripheral blood, and single-cell suspensions from thymus or spleen by direct homogenization in Tri-Reagent (Molecular Research Center, Cincinnati, OH) following the manufacturer's specifications. RNA (15 μg) were electrophoresed on a 1% agarose-formaldehyde gel, blotted onto Hybond-N nylon membrane (Amersham, Arlington Heights, IL), and UV cross-linked. Filters were prehybridized for 4–5 h at 42°C in 5× SSC, 50% formamide, 5× Denhardt's solution, 0.5% SDS, and 10 μg/ml denatured salmon sperm DNA and subsequently hybridized overnight at 42°C in 5× SSC, 50% formamide, 5× Denhardt's solution, 0.5% SDS, and 20 μg/ml denatured salmon sperm DNA. A 2-kb *Eco*RI B-myb fragment corresponding to the most 3′ region of the human B-myb cDNA was purified from plasmid pSV40/B-myb (11), labeled with [α-^{32}P]dCTP using the Random Primed DNA Labeling Kit (Roche, Indianapolis, IN), and used as a human-specific B-myb probe not cross-reacting with murine B-myb. The filters were washed twice with 2× SSC/0.1% SDS at room temperature for 10 min, once at 65°C for 10 min, and twice with 0.2× SSC/0.1% SDS at 65°C for 30 min. The blots were exposed to Kodak X-OMAT XAR5 film at −80°C with intensifying screens. Hybridization to GAPDH cDNA was used as a control for relative RNA loading.

RT-PCR mRNA analysis

Each 20-μl RT reaction contained 10–30 ng RNA, which was incubated at 65°C for 5 min and cooled on ice; 200 μM dNTPs (Roche); 10 mM DTT (Life Technologies); 15 U RNasin (Promega, Madison, WI); 5×10^{-3} U random hexamers (Pharmacia, Piscataway, NJ); 5× first-strand buffer (Life Technologies); and 200 U Moloney murine leukemia virus reverse transcriptase (Life Technologies). The reaction was incubated at 37°C for 90 min.

Each PCR reaction contained 5 μl RT reaction, 200 mM dNTPs, 600 ng reverse primer, 600 ng forward primer, 10× *Taq* buffer (Roche), and 5 U Taq DNA polymerase (Roche) in a total volume of 100 μl. For human B-myb detection, the PCR reaction was run for 30 cycles (30 s at 94°C, 45 s at 62°C, and 30 s at 72°C) with the forward primer, 5′-CGGCAGAGGAAGAGG CGTGTG-3′, corresponding to nt 1361–1381 of human B-myb, and the reverse primer, 5′-CATCATCAGCTTCACATCCTCATC-3′, corresponding to nt 1924–1901. For murine B-myb detection, the PCR reaction was run for 30 cycles (30 s at 94°C, 45 s at 62°C, and 30 s at 72°C) with the forward primer, 5′-GCTAAAGAACTCGGACATGAGCC-3′, corresponding to nt 749–771 of murine B-myb, and the reverse primer, 5′-GATGACTGCAGT GCCTCCTCCT-3′, corresponding to nt 1083–1062. For specific FasL detection, the PCR reaction was run for 15, 20, 22, 25, and 30 cycles (30 s at 94°C, 45 s at 58°C, and 30 s at 72°C) with the forward primer, 5′-ACTGGACA GATATGGGCCCAC-3′, corresponding to nt 821–841 of FasL cDNA, and the reverse primer, 5′-GCCTCTGTGAGGTAGTAAGTAG-3′, corresponding to nt 1342–1321. Murine FasL amplification within the linear range was achieved using 22 PCR cycles. cDNA levels were normalized to those of β-actin amplified using the forward (5′-TGGGAATGGG TCAGAAGGACT-3′) and the reverse (5′-TTTCACGGTTGGCCTTAGGGTT-3′) primers.

Amplification products were run in a 1% agarose gel and transferred to Hybond-N nylon membrane (Amersham) for Southern blot analysis. Human B-myb was detected with an internal ^{32}P end-labeled oligomer, 5′-GAG GAGGACTTGAAGGAGGT-3′, corresponding to nt 1751–1770 of the human B-myb cDNA. Murine FasL was detected with an internal ^{32}P end-labeled oligomer, 5′-AGAGTCTTCTTAAGACCTATTGAGATTAAT-3′, corresponding to nt 1031–1060 of the murine FasL cDNA.

Western blot analysis

Equal numbers of the indicated cells ($5–10 \times 10^6$) were washed twice with ice-cold PBS and lysed directly in SDS sample buffer containing 10% glycerol, 2% SDS, 100 mM Tris (pH 6.5), and 0.2% bromophenol blue. Lysate preparation, SDS-PAGE, transfer to nitrocellulose (Schleicher & Schuell, Keene, NH), membrane blocking, and incubation with primary Ab were performed according to standard procedures (23). The human B-myb protein was detected with a rabbit polyclonal anti-B-myb serum, a gift from Dr. R. E. Lewis (University of Nebraska, Omaha, NE). The anti-mouse FasL rabbit polyclonal serum was obtained from Oncogene Research Products (Cambridge, MA), and the anti-mouse IFN-γ mAb was purchased from BD PharMingen. After incubation with the appropriate secondary Ab conjugated to HRP (Amersham), bound proteins were detected using chemiluminescent substrates according to the manufacturer's instructions (Amersham). Densitometric analysis was performed, and data are reported as densitometric values (mean ± SD).

Cytotoxicity assays

Human Fas$^+$ Jurkat T cells and murine thymocyte Yac-1 cells were used as target cells in 4- or 6-h ^{51}Cr release assays, respectively (24). When indicated, 1 mM EGTA, 2 mM $MgCl_2$, 1 μg/ml human Fas/Fc chimera (R&D Systems), or 1 μg/ml pTAT-HA-DM56/61-BAD fusion protein as a control was added throughout the assay. A constant number of target cells (1×10^4 to 2.5×10^3/well, as indicated) and serial dilutions of effector cells were used in triplicate. ^{51}Cr release (cpm) was determined in a Wallac gamma counter. Spontaneous release (*S*) was measured in wells with target cells alone and was always <10% in the assay. Maximum release (M) was measured from target cells with added 1% Triton X-100. The percentage of specific ^{51}Cr release was calculated as: $[(E - S)/(M - S)] \times 100$, where *E* is ^{51}Cr release from experimental cells. Lytic units were calculated at 15% specific ^{51}Cr release (LU_{15}) and referred to 10^7 cells.

ELISPOT analysis

This was performed as previously described (25). Mice were infected i.p. with 10^7 PFU of the influenza A PR/8/34 virus in 250 μl BSS/BSA or were injected with 250 μl BSS/BSA alone as a control. After 14 days spleens were removed, homogenized, and plated at sequential cell numbers per well in 50 μl assay medium into 96-well ELISPOT plates (Millipore, Bedford, MA). Plates were coated 1 day before the experiment with 20 μg/ml anti-IFN-γ mAb (HB170; American Type Culture Collection, Manassas, VA). The cells were stimulated with 2×10^5 L929 cells transfected to express the H2-K^d molecule (L-K^d) (26), infected with 5 PFU/cell of the influenza A PR/8/3 4 virus in BSS/BSA for 1 h, and then irradiated (10,000 cGy). Uninfected L-K^d cells were used as a control. Plates were incubated at 37°C for 18–24 h, washed extensively, and incubated for 2 h with a biotin-labeled anti-IFN-γ mAb (4 μg/ml; BD PharMingen). After washing, 10 μg/ml HRP-conjugated avidin D (Vector Laboratories, Burlingame, CA) was added to each well, and the plates were incubated for 2 h at room temperature and washed. Single cells producing IFN-γ were detected as spots after addition of 3,3′-diaminobenzidine and β-chloronaphthol dissolved in methanol and added to 10 ml PBS containing 20 μl H_2O_2 (30%). Using a dissecting microscope, spots were counted blindly by two separate investigators.

Results

Generation of tg LCK-B-myb mice

To assess the effects of B-myb expression in lymphoid tissues, the human B-myb cDNA was cloned downstream of the LCK promoter (17) (Fig. 1) and used to obtain B-myb tg mice. Four founders bearing LCK-B-myb were identified by Southern blot analysis of tail DNA (data not shown), and corresponding lines were established. Each line was monitored for B-myb expression by Western and Northern blot analyses of thymus, spleen, and lymph nodes. Three tg LCK-B-myb lines (5986, 6075, and 6085) were further characterized; two (5986 and 6085) were extensively studied.

Human B-myb mRNA expression was detected in the spleen, thymus, and lymph nodes of tg, but not wild-type (wt), mice, as assessed in Northern blot analysis using a human-specific B-myb probe (Fig. 2*A*). Levels of murine B-myb were similar in wt and tg mice, as assessed by RT-PCR analysis of thymus and spleen (Fig. 2*B*), indicating that exogenous human B-myb had no effect on the expression of endogenous murine B-myb. As expected, human B-myb was expressed in T cells, peripheral blood, bone marrow, and NK cells only within transgenic mice; no expression was detected in B cells or macrophages from either wt or transgenic animals (Fig. 2*C*). In Western blot analysis, the transgenic B-myb protein was detected as a 90-kDa B-myb protein in the thymus, spleen (Fig. 2*D*), and lymph nodes (data not shown). Expression in thymus was higher than that in lymph nodes or spleen, consistent with the different percentages of T cells in these organs and with the reportedly more abundant expression of LCK-driven genes in immature than mature T cells (27).

Histologic analysis performed at several time points up to 18 mo of age in two transgenic lines, 5986 and 6085, revealed normal morphology of all lymphoid organs tested (data not shown). No difference was detected between tg and wt mice in the size of the lymphoid organs. Although B-myb overexpression resulted in a small, but statistically significant ($p = 0.02$), decrease in CD3$^+$ splenocytes (33.8 ± 3.6 and 40 ± 3.7 in tg and wt mice, respectively), no significant differences in the proportions of CD4$^+$/CD8$^+$, CD4$^+$, CD8$^+$, NK, NKT (CD3$^+$/Pan-NK$^+$), and B cells in thymus and spleen from 20 tg and five wt mice (Figs. 3 and 4) was detected.

Survival of ex vivo cultures of lymphocytes from B-myb-overexpressing mice

Splenocytes and thymocytes from LCK-B-myb and control mice maintained in complete RPMI 1640 without the addition of cytokines underwent rapid apoptosis. Propidium iodide staining performed on these ex vivo cell cultures at 0, 6, 12, and 24 h revealed that cultures from tg LCK-B-myb thymus and spleen contained more apoptotic cells than those from the corresponding organs of wt animals (Fig. 5). Very low percentages of apoptotic thymocytes and splenocytes were observed at 0 h, before culture. Similar results were obtained, with no measurable differences between tg and wt mice, when apoptotic cells were measured in tissue sections of thymus and spleen by TUNEL assay (data not shown).

FasL expression in LCK-B-myb tg mice

Western blot analysis of total cell extracts from thymus and spleen of tg and wt animals (Fig. 6*A*) revealed significantly higher levels of FasL in both splenocytes and thymocytes from tg than wt mice. In spleen cells two bands were detected reacting with the anti-FasL mAb. The relative mass of the largest band (~35–43 kDa) corresponds to that of full-length FasL, while the smaller (~26 kDa) corresponds to that reported for truncated FasL (membrane shed and lysosome secreted). Both forms were expressed more abundantly in splenocytes from tg than wt mice. Densitometric values for full-length and truncated FasL in tg splenocytes were 158 ± 18 and 186 ± 17 compared with 85 ± 10 and 73 ± 13 for wt cells, respectively ($n = 3$). In cell extracts from thymocytes, only the full-length FasL protein was detectable, and, as in splenocytes, its levels were more abundant in cells from tg than wt mice. The densitometric value for full-length FasL in transgenic thymocytes

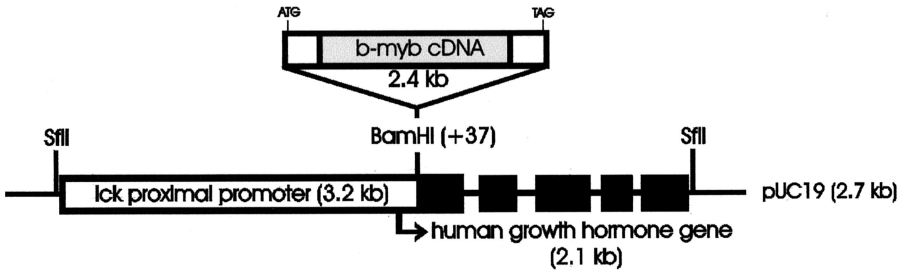

FIGURE 1. LCK-B-myb transgene construct. A 2.4-kb (▨) human B-myb cDNA was inserted at the *Bam*HI site downstream of the 3.2-kb LCK proximal promoter (□). Introns, exons, and polyadenylation sites (■) of the human growth hormone gene constitute the 3′-untranslated region.

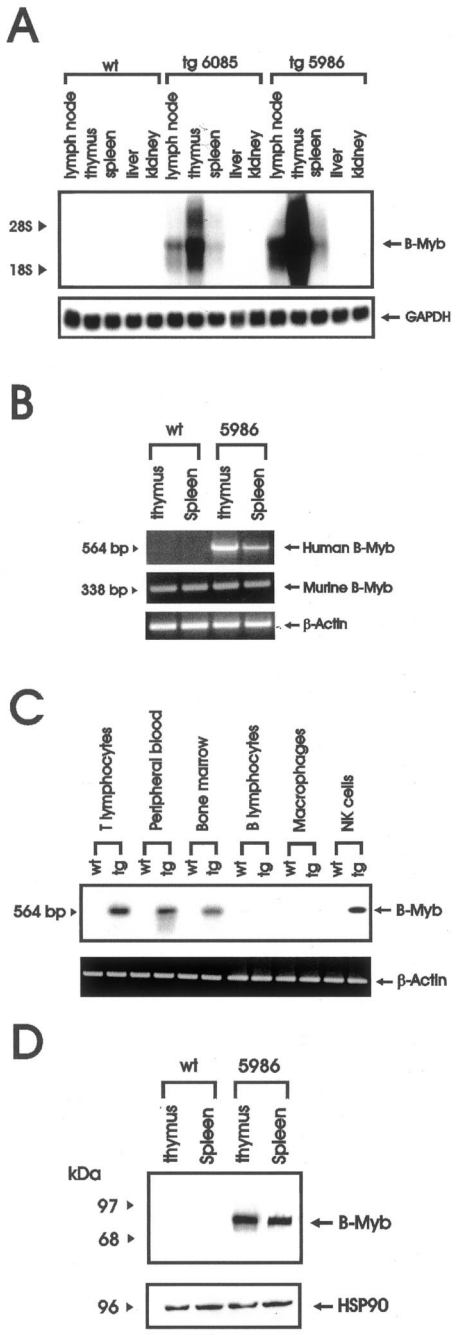

FIGURE 2. B-myb expression in transgenic LCK-B-myb mice. *A*, Human B-myb mRNA expression was analyzed (Northern blot) in the indicated organs from wt and the indicated lines of LCK-B-myb tg mice. GAPDH mRNA was measured to control for RNA loading. *B*, RT-PCR analysis of human (*top*) and murine (*bottom*) B-myb mRNA from thymus and spleen of wt and LCK-B-myb tg mice. β-Actin transcripts were amplified for normalization. Oligonucleotide primers are described in *Materials and Methods*. *C*, RT-PCR analysis of human B-myb mRNA from the indicated cell types of wt and LCK-B-myb tg mice. T, B, and NK cells were isolated from the spleen. RT-PCR products were obtained using human B-myb-specific oligonucleotide primers and were hybridized to a ^{32}P end-labeled human B-myb-specific oligo probe. β-Actin transcripts were amplified for normalization. *D*, Western blot analysis of total thymus and spleen extracts from non-tg wt and LCK-B-myb tg mice (5986). Analysis was performed on an equivalent number of cells using polyclonal rabbit anti-B-myb Ab (Lewis). A mouse anti-heat shock protein 90 (HSP90) mAb was used to control for protein loading.

was 62 ± 13 compared with 28 ± 9 for wt cells, respectively ($n = 3$).

To investigate whether the elevated levels of FasL protein in cells from tg mice corresponded to increased mRNA levels, semiquantitative RT-PCR analysis was performed on RNA isolated from thymocytes and splenocytes of tg and wt mice (Fig. 6*B*). Levels of FasL mRNA were similar in tg and wt thymocytes, but were markedly increased in tg splenocytes compared with those in cells from control mice. Also, FasL mRNA levels were more abundant in tg than in wt spleen T and NK cells purified to homogeneity by cell sorting (Fig. 6*C*).

IFN-γ expression in LCK-B-myb tg mice

Increased FasL expression suggested activation of T and/or NK cells. We investigated whether other signs of activation, such as production of cytokines, could be detected. ELISPOT analysis was used to determine the number of spontaneous and virus-specific IFN-γ-producing splenocytes (Fig. 7*A*). Splenocytes from influenza virus-infected and noninfected mice were restimulated in vitro with infected or noninfected syngeneic L-K^d APCs to compare the frequency of spontaneous and virus-specific IFN-γ production. Splenic lymphocytes from wt mice contained a very low number of cells producing IFN-γ spontaneously, that is, production by splenocytes stimulated with noninfected L-K^d cells. The number was only slightly higher when splenocytes from virus-infected mice were used, indicating a minimal secondary response in the absence of specific stimulation with the virus. The number of IFN-γ-producing cells was increased 10-fold when wt splenocytes from virus-infected mice were restimulated with infected L-K^d cells compared with that in response to noninfected L-K^d cells and the primary in vitro response of splenocytes from noninfected mice to virus-infected L-K^d cells. A significantly greater number of lymphocytes from tg mice spontaneously produced IFN-γ, whether from virus-infected or noninfected mice, compared with those from wt mice. The frequency of IFN-γ-producing cells in the specific primary and secondary responses to in vitro stimulation with infected L-K^d cells was also greater in tg compared with wt mice, although there was only a 4-fold increase in virus-specific vs spontaneous IFN-γ-producing splenocytes.

Western blot analysis performed on total spleen extracts of tg and wt animals confirmed that the levels of the 20-kDa IFN-γ protein were higher in spleen cells from LCK-B-myb tg than control mice (Fig. 7*B*).

T and NK cell-mediated cytotoxicity in LCK-B-myb tg mice

Splenic lymphocytes from tg mice mediated significantly higher cytotoxicity than those from wt mice against the Fas$^+$ Jurkat cell line (Fig. 8*A*). Low cytotoxicity mediated by wt cells against Jurkat target cells, sensitive to both Fas and granule exocytosis-mediated cytotoxicity, was only marginally inhibited by EGTA, which prevents exocytosis-mediated cytotoxicity by inhibiting perforin (PFP) polymerization and membrane pore formation and was almost completely inhibited in the presence of a recombinant human Fas (rhFas) chimera protein. For wt cells, $LU_{15}/10^7$ cells were reduced from 87 to 60 and 18, respectively. In contrast, significantly higher cytotoxicity was mediated by splenocytes from the tg mice, which was unexpectedly inhibited by EGTA from 313 to 125 $LU_{15}/10^7$ cells. The rhFas chimeric protein inhibited almost completely the remaining cytotoxicity to 28 $LU_{15}/10^7$ cells. These data are consistent with a higher cytotoxic potential of the transgenic lymphocytes compared with the wt cells.

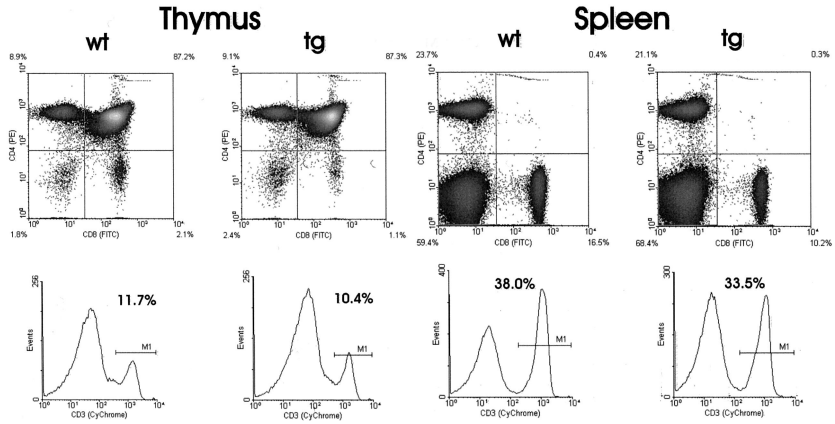

FIGURE 3. Lymphocyte subsets in spleen and thymus. Lymphocyte subsets were analyzed in thymus (*left*) and spleen (*right*) from wt and tg, 5986, mice. CD4, CD8, and CD3 expressions were detected by three-color immunofluorescence as described in *Materials and Methods*, using PE-conjugated anti-CD4, FITC-conjugated anti-CD8, and CyChrome-conjugated anti-CD3. Lymphocytes were gated on the basis of light scatter characteristics. Correlate measurements of FITC (*x*-axis) and PE (*y*-axis) were performed on gated CyChrome anti-CD3$^+$ cells and are displayed as density plots on 4-decade $\log_{10}$ scales. Based on negative controls with irrelevant Ab (not shown), the plots were divided into quadrants in which $<0.5\%$ control cells were included. The percentage of positive cells is reported for each quadrant. *Top left*, PE only positive cells; *top right*, double-positive cells; *bottom right*, FITC only positive cells. The *bottom panels* in each section are histograms of cells reacting with CyChrome anti-CD3 Ab in the total population. The percentage of positive cells is indicated. *x*-axis, Fluorescence intensity; *y*-axis, relative cell number. Results are from one experiment using one mouse and are representative of 5 wt and 20 tg mice analyzed.

Cytotoxicity assays were performed with total splenic lymphocytes against the NK-sensitive YAC-1 target cells (28). The cytotoxic activity of NK cells from the LCK-B-myb tg mice was significantly higher than that of the cells from wt mice (322 vs 18 $LU_{15}/10^7$ cells, respectively; Fig. 8*B*).

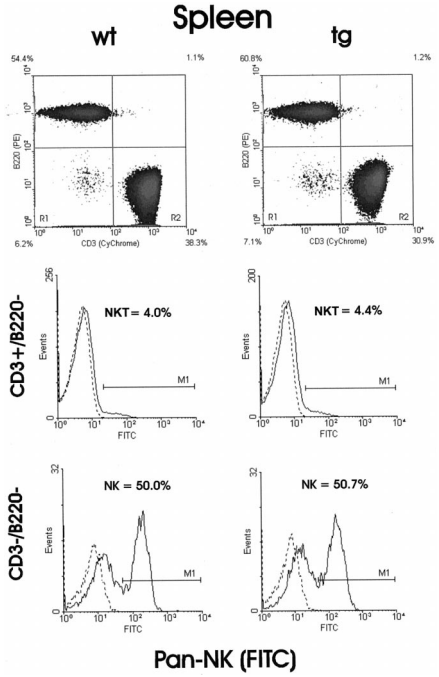

FIGURE 4. B, T, NK, and NKT subsets in spleen. Lymphocyte subsets were analyzed in spleen from wt and tg, 5986, mice. B220, CD3, and Pan-NK expressions were detected by three-color immunofluorescence as described in Fig. 3, using PE-conjugated anti-B220, FITC-conjugated anti-Pan-NK, and CyChrome-conjugated anti-CD3. The *bottom panels* in each section indicate cells reacting with FITC anti-Pan-NK mAb within gated CD3$^+$/B220$^-$ and CD3$^-$/B220$^-$ lymphocytes. The percentage of positive cells within the gated population is indicated. *x*-axis, Fluorescence intensity; *y*-axis, relative cell number. Results are from one experiment using one mouse and are representative of five wt and 20 tg mice analyzed.

To further determine whether only NK or both T and NK cells from tg mice mediate higher levels of Fas/FasL-dependent killing, purified T and NK cells were used in 6-h ^{51}Cr release assays with Jurkat as target cells in the presence of EGTA and either rhFas chimeric protein or an irrelevant chimeric protein as a control (Fig. 8, *C* and *D*, NK and T cells, respectively). Cytotoxicity of NK cells from transgenic mice was reduced from 278 to 90 $LU_{15}/10^7$ cells compared with 179 and 59 $LU_{15}/10^7$ cells for wt NK cells. Similarly, transgenic T cell cytotoxicity was reduced from 53 to 25 compared with 13 and 3 $LU_{15}/10^7$ cells for wt T cells. Both T and NK cells from transgenic mice mediated levels of cytotoxicity higher than those from wt mice, and in both cases their effects were significantly inhibited by the rhFas chimera.

Discussion

B-myb expression is up-modulated during the G_1/S transition in peripheral blood T cells and results in enhanced survival of

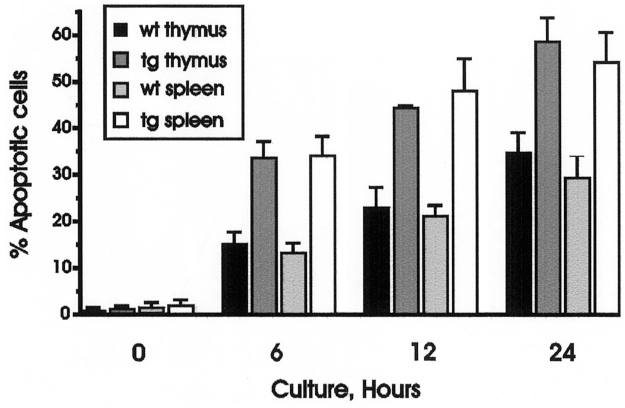

FIGURE 5. Viability of thymus and spleen cells from tg LCK-B-myb mice. Thymocytes and splenocytes from wt and LCK-B-myb tg mice were cultured in RPMI 1640 without the addition of growth factors or cytokines. The percentage of apoptotic cells was determined by DNA content analysis of PI-stained nuclei at 0, 6, 12, and 24 h. Bars and error bars are the mean ± SD of the results from three independent experiments.

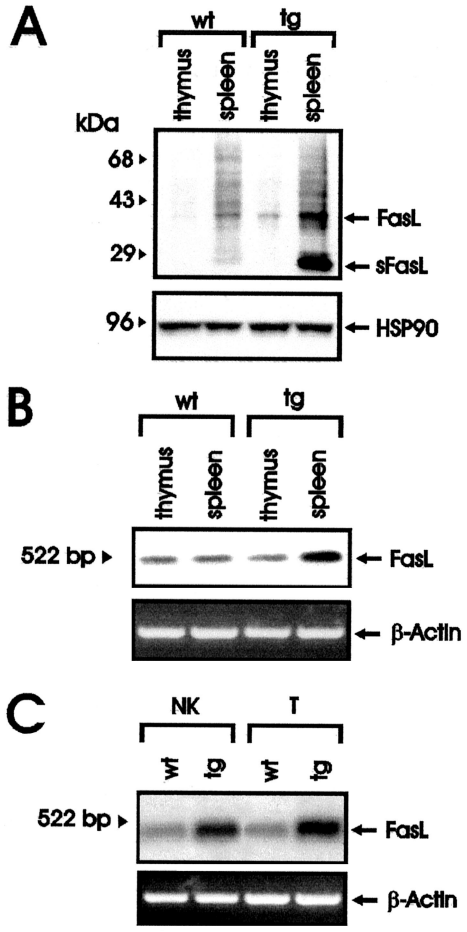

FIGURE 6. FasL expression in tg LCK-B-myb mice. *A*, Western blot analysis of total thymus and spleen extracts from wt and tg LCK-B-myb mice. Analysis was performed on an equivalent number of cells using polyclonal rabbit anti-FasL Ab for detection. The 35/43-kDa band corresponds to full-length FasL; the 26-kDa band corresponds to truncated, soluble FasL (sFasL). Mouse anti-heat shock protein 90 (HSP90) mAb was used to control for protein loading. *B*, Semiquantitative RT-PCR analysis of FasL mRNA from thymus and spleen of wt and tg LCK-B-myb mice. RT-PCR products obtained using FasL-specific oligonucleotide primers were hybridized to a ^{32}P-end-labeled FasL-specific oligo probe. The expected 522-bp RT-PCR product corresponding to FasL is indicated. The RT-PCR reaction was performed with 22 cycles; oligonucleotide primers and oligo probe are detailed in *Materials and Methods*. The results are from one experiment representative of three independent ones performed. β-Actin transcripts were amplified for normalization. *C*, Semiquantitative RT-PCR analysis of FasL mRNA from NK and T cells purified to homogeneity from spleen of wt and tg LCK-B-myb mice. RT-PCR analysis was performed as described in *B*.

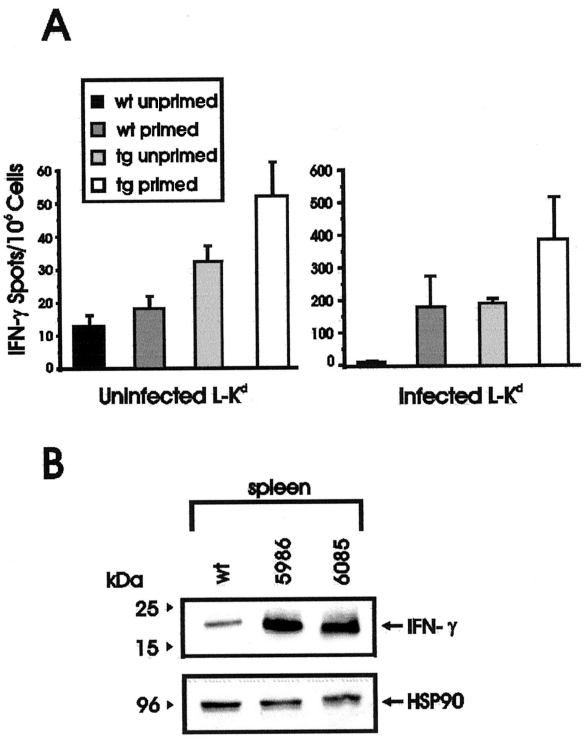

FIGURE 7. IFN-γ production in transgenic LCK-B-myb mice. *A*, IFN-γ ELISPOT assay with splenic lymphocytes from wt and tg LCK-B-myb mice. Assays were performed 14 days after priming i.p. with influenza A PR/8/34 virus (10^7 PFU/mouse). Unprimed mice and uninfected L-K^d cells were used as controls. The number of spontaneous (*left*) and A PR/8/34-specific (*right*) IFN-γ-producing cells/10^6 splenocytes is shown. Bars and error bars are the mean $\pm$ SD of three independent experiments. *B*, Western blot analysis of total spleen extracts from wt and LCK-B-myb tg, 5986 and 6085, mice. Analysis was performed with an equivalent number of splenocytes using rat anti-IFN-γ mAb. The 20-kDa band corresponding to IFN-γ is indicated. Mouse anti-heat shock protein 90 (HSP90) mAb was used to control for protein loading.

CTLL-2 cells at least in part through bcl-2 induction (14, 29), suggesting a possible role for B-myb in T cell survival, proliferation, and activation. To evaluate this in vivo, we generated tg mice expressing human B-myb in their T and NK cell lineages using the proximal LCK promoter.

LCK-B-myb tg mice express the transgene in T and NK cells, but as expected, not in B or myeloid cells. B-myb expression in NK cells, defined by RT-PCR, is not due to amplification from contaminating T cells because no CD3-γ amplification, detected in T cells, was obtained using cDNA from purified NK cells (data not shown). These data indicate that the proximal LCK promoter is functional in NK cells, which has not been previously reported in the murine model system. However, it is known that p56^{lck} is expressed in both human and murine NK cells, and its activity is essential for signal transduction via FcγRIIIA in these cells (30).

The survival of tg and wt mice was identical, and no signs of disease or changes in behavior were observed in LCK-B-myb mice. Gross and microscopic examination of the lymphoid organs from two LCK-B-myb transgenic lines revealed no abnormalities in size and histology in mice up to 18 mo of age. Although a small decrease in the percentages of CD3$^+$ cells was observed in the spleen of tg mice, the possible biological significance of this finding remains unclear because the relative proportions of CD4$^+$/CD8$^+$, CD4$^+$, and CD8$^+$ and of all other lymphoid subsets were unchanged between wt and tg mice.

In agreement with normal morphology of lymphoid organs, TUNEL staining revealed no significant difference in the frequency of apoptotic cells in vivo in tissue sections from thymus and spleen of tg and wt mice (data not shown), consistent with the very low percentage of apoptotic cells in these organs before ex vivo cell culture in medium not supplemented with growth factors. However, cell cycle analysis indicated that thymocytes and splenocytes from LCK-B-myb tg mice survive in culture without stimulation for shorter time than the corresponding wt cells.

Fas/FasL-mediated apoptotic cell death is central to the development of the immune system (31, 32), and FasL expression upon T cell activation limits the expansion of T cell clones after Ag elimination and is involved in inducing peripheral tolerance (33). No difference in Fas expression was detected between tg and wt mice (data not shown). Instead, the results of Western blot analysis

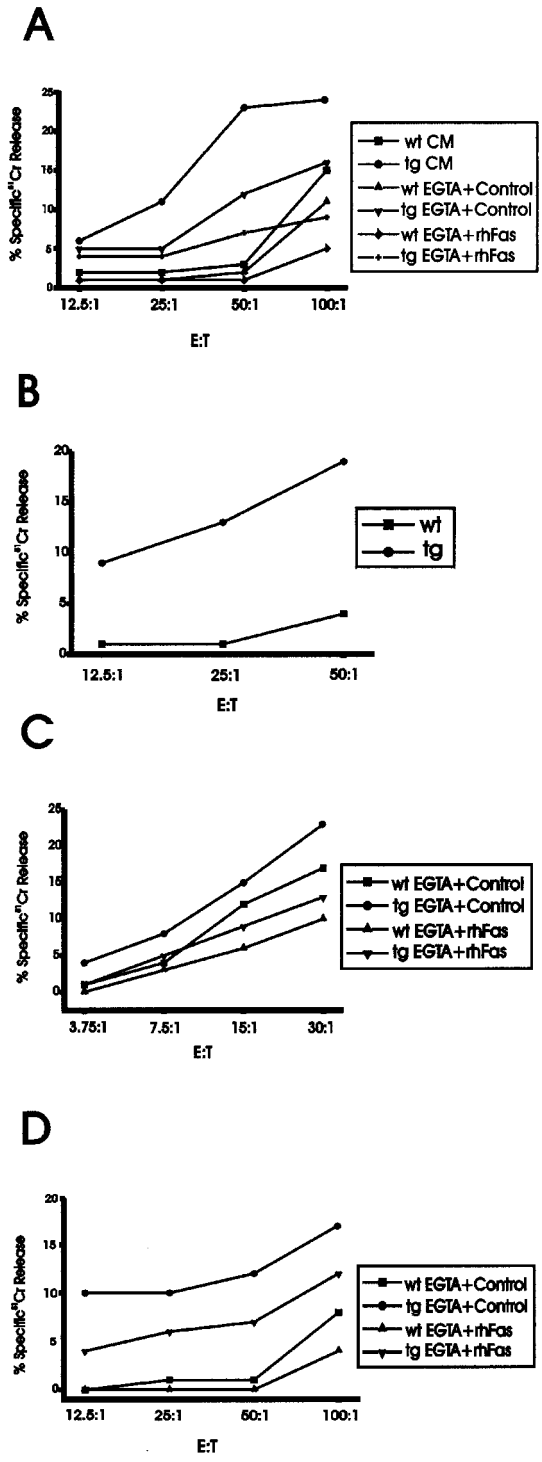

FIGURE 8. T and NK cell-mediated cytotoxicity. *A*, Cytotoxicity assays were performed in complete medium (CM) with or without added 1 mM EGTA and 2 mM $MgCl_2$ and Fas/Fc chimera or a control fusion protein (TAT-HA mutant BAD), as indicated, with cells from wt and tg mice. Jurkat cells (10^4/well) were used as targets in 6-h ^{51}Cr release assays. Effector cells were splenic lymphocytes. *B*, Yac-1 cells (10^4/well) were used as targets in 4-h ^{51}Cr release assays. Effector cells were splenic lymphocytes. *C* and *D*, Jurkat cells (2.5×10^3/well) were used as targets in 6-h ^{51}Cr release assays. Effector cells in C were NK cells purified to homogeneity from spleen by cell sorting. Effector cells in D were T cells purified by panning (negative selection). Results are from one experiment using one mouse and are representative of three independent ones with each cell type. *x*-axis, E:T cell ratio; *y*-axis, percentage of specific ^{51}Cr release.

indicated that thymocytes, splenocytes, and specifically, T and NK cells from tg mice expressed higher levels of FasL than those from wt mice. Upon incubation of ex vivo cultured B-myb-expressing thymocytes and splenocytes with rhFas chimera protein, apoptosis was in part inhibited (data not shown), suggesting that a Fas/FasL-mediated mechanism possibly contributes to the increased apoptosis of these cells in vitro. This and the fact that T cells are sensitive to Fas-induced apoptosis in a suicide fashion (34, 35) may explain the observation that mature $CD3^+$ splenocytes are slightly decreased in the spleen of LCK-B-myb transgenics.

The increased levels of FasL in lymphocytes from the B-myb tg T and NK cells may reflect or be a consequence of activation upon B-myb expression (33). We tested this hypothesis by analyzing cytokine production and spontaneous cytotoxicity. The results of ELISPOT and Western blot analysis indicate that the levels of IFN-γ in the spleen from nonstimulated tg mice are higher than those in wt mice. Also, the frequency of lymphocytes producing IFN-γ in the absence of in vitro or in vivo viral stimulation was significantly greater than that in wt mice. IFN-γ is produced by all lymphocyte subsets in which the B-*myb* transgene is expressed, i.e., T, NK, and probably ($CD3^+$/Pan-NK^+) NKT cells. Thus, our results may simply be explained based on increased IFN-γ production by any or all of these cell types. We observed a 4- and 2-fold increase in the number of IFN-γ-producing unprimed and in vivo primed transgenic cells, respectively, whereas a 10-fold increase in both was observed with wt mice. We consider it unlikely that this depends on a lower responsiveness of the tg cells to stimulation of IFN-γ. Rather, we propose that when stimulated, wt and tg cells have a similar increase in IFN-γ production; however, IFN-γ production might be masked in the tg animals because of the increased basal number of IFN-γ-producing cells.

The mechanism(s) responsible for increased IFN-γ expression/production might involve lineage-specific direct effects of B-myb on IFN-γ transcription or effects on the expression of cytokines inducing production of IFN-γ. Among these, IL-12, -15, and -18, potent inducers of IFN-γ, are produced exclusively by accessory nonlymphoid cells, not expressing the transgene, making their role unlikely in our tg mice. Rather, the possibility that B-myb expression affects IL-2 and/or IL-4 production by B-myb-expressing T and/or NKT cells is more likely and needs to be analyzed.

NK and T cells play a pivotal role in host defense. The effector role of NK cells in innate resistance is mediated in part via cytokine production, particularly IFN-γ, and in part via direct target cell killing (36–38). NK and T cell-mediated cytotoxicity occurs through two major pathways: granule exocytosis of the cytotoxic molecules PFP and granzymes, and TNF/TNF receptor family members (33, 39). Splenic lymphocytes from tg mice were more potent effectors of cytotoxicity than wt cells both against Jurkat (Fas^+) and Yac-1 (Fas^-, NK sensitive) target cells, indicating that B-myb expression also results in increased cytotoxicity. Yac-1 cells are sensitive only to NK cells and PFP-mediated lysis (28). PFP was detected at similar levels (Western blot analysis, data not shown) in wt and tg T and NK cells, making it unlikely that the increased granule-mediated cytotoxicity of NK cells depends on increased PFP usage. Activating, target-binding receptors have been recently identified in human cytokine-activated NK and T cells (40), and we favor the possibility that other activation-dependent factors, such as an increase in target cell recognition

 0022-1767/01/$02.00

and/or adhesion molecules, are involved in the increased cytotoxicity of B-myb transgenic NK cells.

Resting T cells are not cytotoxic and do not express PFP. Thus, it could be expected that the increased level of cytotoxicity mediated by T cells against the Fas^+ Jurkat cells depends exclusively on increased FasL expression and is FasL mediated. Surprisingly, tg T cell cytotoxicity was inhibited in the absence of Ca^{2+}. As for NK cells, it is unlikely that this is caused by B-myb-dependent PFP expression, and the data are not in contrast with the possibility that most, if not all, cytotoxicity mediated by the tg T cells is FasL dependent. Our data indicate an increased expression of the lower molecular mass, truncated form of FasL, which is known to be nonmembrane bound, stored in specialized secretory lysosomes in monocytes and T and NK cells, and released or shed from the cell surface (41–43) upon target cell interaction. If FasL release from these granules, like most exocytosis processes, is Ca^{2+} dependent, degranulation is probably inhibited in the absence of Ca^{2+}. In this case the inhibition of tg T and NK cells cytotoxicity by EGTA may depend on inhibition of FasL release.

In summary, increases in IFN-γ and FasL expression as well as cytotoxicity are all indicative of lymphocyte activation in B-myb-overexpressing T and NK cells. The exact mechanism by which B-myb expression results in this activation remains to be determined. Our preliminary data (not shown) suggest that B-myb does not induce increased transcription of FasL and IFN-γ directly. Therefore, B-myb may act indirectly by affecting the expression of other factors in T and/or NK cells that induce activation or are involved in regulating IFN-γ and FasL expression. Alternatively, B-myb may in part regulate IFN-γ and FasL at a post-transcriptional level. Regardless of the mechanism(s) involved, B-myb tg mice provide a useful in vivo model to study the regulation and NK and T cell activation and cytotoxicity.

Acknowledgments

We thank Jason McCormick, Flow Cytometry Facility, for assistance with cell sorting, and Dr. Linda Siracusa and the personnel of the Transgenic Animal Facility for generation of transgenic mice.

References

1. Lyon, J., C. Robinson, and R. Watson. 1994. The role of Myb proteins in normal and neoplastic cell proliferation. *Crit. Rev. Oncog. 5:373.*
2. Introna, M., M. Luchetti, M. Castellano, M. Arsura, and J. Golay. 1994. The myb oncogene family of transcription factors: potent regulators of hematopoietic cell proliferation and differentiation. *Semin. Cancer Biol. 5:113.*
3. Nakagoshi, H., Y. Takemoto, and S. Ishii. 1993. Functional domains of the human B-myb gene product. *J. Biol. Chem. 268:14161.*
4. Saville, M. K., and R. J. Watson. 1998. B-Myb: a key regulator of the cell cycle. *Adv. Cancer Res. 72:109.*
5. Weston, K. 1998. Myb proteins in life, death and differentiation. *Curr. Opin. Genet. Dev. 8:76.*
6. Toscani, A., R. V. Mettus, R. Coupland, H. Simpkins, J. Litvin, J. Orth, K. S. Hatton, and E. P. Reddy. 1997. Arrest of spermatogenesis and defective breast development in mice lacking A-myb. *Nature 386:713.*
7. Mucenski, M. L., K. McLain, A. B. Kier, S. H. Swerdlow, C. M. Schreiner, T. A. Miller, D. W. Pietryga, W. J. Scott Jr., and S. S. Potter. 1991. A functional c-myb gene is required for normal murine fetal hepatic hematopoiesis. *Cell 65: 677.*
8. Tanaka, Y., N. P. Patestos, T. Maekawa, and S. Ishii. 1999. B-myb is required for inner cell mass formation at an early stage of development. *J. Biol. Chem. 274: 28067.*
9. Watson, R. J., C. Robinson, and E. W. Lam. 1993. Transcription regulation by murine B-myb is distinct from that by c-myb. *Nucleic Acids Res. 21:267.*
10. Sala, A., and R. Watson. 1999. B-Myb protein in cellular proliferation, transcription control, and cancer: latest developments. *J. Cell Physiol. 179:245.*
11. Sala, A., and B. Calabretta. 1992. Regulation of BALB/c 3T3 fibroblast proliferation by B-myb is accompanied by selective activation of cdc2 and cyclin D1 expression. *Proc. Natl. Acad. Sci. USA 89:10415.*
12. Lin, D., M. Fiscella, P. M. O'Connor, J. Jackman, M. Chen, L. L. Luo, A. Sala, S. Travali, E. Appella, and W. E. Mercer. 1994. Constitutive expression of B-myb can bypass p53-induced Waf1/Cip1-mediated G1 arrest. *Proc. Natl. Acad. Sci. USA 91:10079.*
13. Golay, J., V. Broccoli, G. M. Borleri, E. Erba, M. Faretta, L. Basilico, G. G. Ying, G. Piccinini, L. H. Shapiro, J. Lovric, et al. 1997. Redundant functions of B-Myb and c-Myb in differentiating myeloid cells. *Cell Growth Differ. 8:1305.*
14. Grassilli, E., P. Salomoni, D. Perrotti, C. Franceschi, and B. Calabretta. 1999. Resistance to apoptosis in CTLL-2 cells overexpressing B-Myb is associated with B-Myb-dependent bcl-2 induction. *Cancer Res. 59:2451.*
15. Bies, J., and L. Wolff. 1995. Acceleration of apoptosis in transforming growth factor β1-treated M1 cells ectopically expressing B-myb. *Cancer Res. 55:501.*
16. Raschella, G., A. Negroni, A. Sala, S. Pucci, A. Romeo, and B. Calabretta. 1995. Requirement of b-myb function for survival and differentiative potential of human neuroblastoma cells. *J. Biol. Chem. 270:8540.*
17. Chaffin, K. E., C. R. Beals, T. M. Wilkie, K. A. Forbush, M. I. Simon, and R. M. Perlmutter. 1990. Dissection of thymocyte signaling pathways by in vivo expression of pertussis toxin ADP-ribosyltransferase. *EMBO 9:3821.*
18. Hogan, B., F. Constantini, and E. Lacy. 1996. *Manipulating the Mouse Embryo: A Laboratory Manual*. Cold Spring Harbor Laboratory Press, Cold Spring Harbor.
19. Mage, M. G., L. L. McHugh, and T. L. Rothstein. 1977. Mouse lymphocytes with and without surface immunoglobulin: preparative scale separation in polystyrene tissue culture dishes coated with specifically purified anti-immunoglobulin. *J. Immunol. Methods 15:47.*
20. Wysocki, L. J., and V. L. Sato. 1978. "Panning" for lymphocytes: a method for cell selection. *Proc. Natl. Acad. Sci. USA 75:2844.*
21. Falabella, F. 1967. Bleeding mice: a successful technique of cardiac puncture. *J. Lab. Clin. Med. 70:981.*
22. Kaplan, H. M. 1973. Cardiac puncture in laboratory animals. *Lab. Anim. Sci. 23:131.*
23. Sambrook, J., E. F. Fritsch, and T. Maniatis. 1984. *Molecular Cloning: A Laboratory Manual*. Cold Spring Harbor Laboratory Press, Cold Spring Harbor.
24. Zamai, L., M. Ahmad, I. M. Bennett, L. Azzoni, E. S. Alnemri, and B. Perussia. 1998. Natural killer (NK) cell-mediated cytotoxicity: differential use of TRAIL and Fas ligand by immature and mature primary human NK cells. *J. Exp. Med. 188:2375.*
25. Miyahira, Y., K. Murata, D. Rodriguez, J. R. Rodriguez, M. Esteban, M. M. Rodrigues, and F. Zavala. 1995. Quantification of antigen specific $CD8^+$ T cells using an ELISPOT assay. *J. Immunol. Methods 181:45.*
26. Eisenlohr, L. C., I. Bacik, J. R. Bennink, K. Bernstein, and J. W. Yewdell. 1992. Expression of a membrane protease enhances presentation of endogenous antigens to MHC class I-restricted T lymphocytes. *Cell 71:963.*
27. Reynolds, P. J., J. Lesley, J. Trotter, R. Schulte, R. Hyman, and B. M. Sefton. 1990. Changes in the relative abundance of type I and type II lck mRNA transcripts suggest differential promoter usage during T-cell development. *Mol. Cell. Biol. 10:4266.*
28. Stewart, I. J. 1994. Granulated metrial gland cells–not part of the natural killer cell lineage? *J. Reprod. Immunol. 26:1.*
29. Reiss, K., S. Travali, B. Calabretta, and R. Baserga. 1991. Growth regulated expression of B-myb in fibroblasts and hematopoietic cells. *J. Cell. Physiol. 148:338.*
30. Salcedo, T. W., T. Kurosaki, P. Kanakaraj, J. V. Ravetch, and B. Perussia. 1993. Physical and functional association of $p56^{lck}$ with FcγRIIIA (CD16) in natural killer cells. *J. Exp. Med. 177:1475.*
31. Golab, J. 2000. Interleukin 18-interferon γ inducing factor–a novel player in tumour immunotherapy? *Cytokine 12:332.*
32. Niho, Y., and Y. Asano. 1998. Fas/Fas ligand and hematopoietic progenitor cells. *Curr. Opin. Hematol. 5:163.*
33. Waring, P., and A. Mullbacher. 1999. Cell death induced by the Fas/Fas ligand pathway and its role in pathology. *Immunol. Cell. Biol. 77:312.*
34. Nagata, S. 1999. Fas ligand-induced apoptosis. *Annu. Rev. Genet. 33:29.*
35. Pinkoski, M. J., and D. R. Green. 1999. Fas ligand, death gene. *Cell Death Differ. 6:1174.*
36. Boehm, U., T. Klamp, M. Groot, and J. C. Howard. 1997. Cellular responses to interferon-γ. *Annu. Rev. Immunol. 15:749.*
37. Trinchieri, G. 1989. Biology of natural killer cells. *Adv. Immunol. 47:187.*
38. Liu, C.-C., and B. Perussia. Natural killer cells: molecular basis of cytotoxic effector functions and their development. In *NK Cells and Cancer: Biology and Therapy*. W. Chambers, ed. *In press.*
39. Lowin, B., M. C. Peitsch, and J. Tschopp. 1995. Perforin and granzymes: crucial effector molecules in cytolytic T lymphocyte and natural killer cell-mediated cytotoxicity. *Curr. Top. Microbiol. Immunol. 198:1.*
40. Moretta, A., C. Bottino, M. Vitale, D. Cantoni, M. C. Mingari, L. M. Moretta. 2001. Activating receptors and coreceptors involved in human natural killer cell-mediated cytolysis. *Annu. Rev. Immunol. 19:197.*
41. Kiener, P. A., P. M. Davis, B. M. Rankin, S. J. Klebanoff, J. A. Ledbetter, G. C. Starling, and W. C. Liles. 1997. Human monocytic cells contain high levels of intracellular Fas ligand: rapid release following cellular activation. *J. Immunol. 159:1594.*
42. Kayagaki, N., A. Kawasaki, T. Ebata, H. Ohmoto, S. Ikeda, S. Inoue, K. Yoshino, K. Okumura, and H. Yagita. 1995. Metalloproteinase-mediated release of human Fas ligand. *J. Exp. Med. 182:1777.*
43. Bossi, G., and G. M. Griffiths. 1999. Degranulation plays an essential part in regulating cell surface expression of Fas ligand in T cells and natural killer cells. *Nat. Med. 5:90.*